Pipeline Response to Undermining at Excavation Crossings

HARRY E. STEWART AND THOMAS D. O'ROURKE

A series of field tests was conducted to investigate the response of cast-iron pipelines subjected to cross-trench construction and to identify conditions that might lead to brittle failure. Static strains were measured for various trench widths, backfill conditions, and both static and dynamic construction vehicle loadings. Tests also were conducted to evaluate the increases in rolling wheel loads that would be caused by surface irregularities. Design recommendations for maximum excavation width and a limiting pipeline strain of 500 microstrain are presented. The recommendations consider the static response of the pipe during backfill and construction vehicle loadings as well as the dynamic response following restoration of the roadway. Design recommendations for maximum allowable trench widths are given for 102-, 152-, and 203-mm diameter cast-iron pipelines that have depths of burial from 0.6 to 1.5 m.

The vulnerability of pipelines and conduits to undermining excavations is dominated by the most vulnerable piping materials. Among the most brittle and aged piping in the U.S. infrastructure are cast-iron pipelines, which are critical for water supplies and gas distribution systems. Although cast-iron piping has provided consistent and dependable service for many years, it is nonetheless a brittle material that fails at strains substantially less than those damaging the ductile pipe materials in modern installations.

Because cast-iron pipelines frequently are undermined by trench construction for other utilities, it is of considerable importance to understand the mechanics of soil-pipeline interaction under these conditions. Special field testing was conducted at a site near Cornell University to investigate pipeline response to cross-trench construction (*1*). The tests were organized to assess pipeline strains caused by backfilling and construction vehicle loads.

The experimental setup and field measurements are described here, and the static strains measured for various trench widths, truck wheel loads, and the locations of cast-iron joints with respect to the loads are reported. The development and verification by experimental data of theoretical models to predict pipeline response are discussed, followed by an explanation of how pipeline deformations under static and dynamic loading were combined to provide a comprehensive model for engineering and planning. Recommendations are made pertaining to the maximum width of cross-trench construction for maintaining pipeline integrity, based on the theoretical models and field test verification program.

School of Civil and Environmental Engineering, Cornell University, Ithaca, N.Y. 14853-3501.

EXPERIMENTAL SETUP

The location and soil conditions at the field test site are described. Detailed information pertaining to the regional setting and geology, characteristics of the soil profile at site, and laboratory tests for soil classification are given elsewhere (*1*).

Soil Profile

A typical soil profile for the test site consisted of approximately 25 to 50 mm of asphalt overlying approximately 200 to 250 mm of a subbase composed of glacial till. In general, at depths greater than 0.3 m and up to 2.7 m, the predominant soil was a heterogeneous mixture of silt, clay, sand, gravel, and cobbles, which is typical of glacial till. Rock consisting mainly of shale and sandstone was encountered at a depth of approximately 2.7 m. The water table was located approximately 1.2 to 2.0 m below the ground surface.

The material used to backfill the pipeline was a poorly graded, coarse-to-medium fluvial glacial sand. It was composed by weight of approximately 99 percent sand and approximately 1 percent fine-grained material. This material was selected because it is similar to select backfill often used in pipeline construction. The moisture-density relationship of the sand backfill was determined according to ASTM D698-78. The optimum moisture content was found to be approximately 10 percent, with a corresponding dry unit weight of 18.8 kN/m^3.

Backfilling, Pipe Installation, and Surfacing

A profile view of the soil and pavement at the test pipeline is shown in Figure 1(*a*). A plan view of the site, which also outlines the north and south test bays, is shown in Figure 1(*b*). The in situ material was excavated to a minimum depth of 1.2 m in the areas outside the two test bays and was removed to a minimum 1.8-m depth within the two test bay areas. The test bays were the locations where the trenches were excavated perpendicular to the experimental pipeline. The trenches for the pipeline and test bays were backfilled with sand in 150- to 200-mm lifts and compacted. The backfill was compacted at a water content of 7 percent and to a relative compaction (RC) of 93 percent. The pipeline was installed so that the top of the pipe was approximately 0.75 m below the top of pavement. The trench then was backfilled with sand to a depth approximately 380 mm below the top of the pavement.

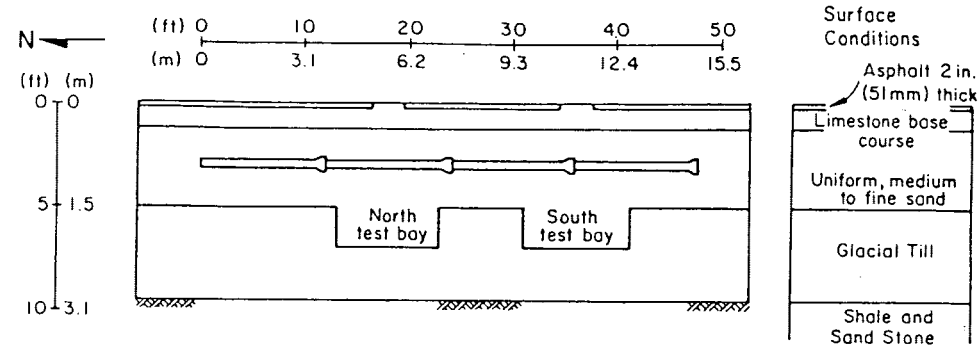

(a)

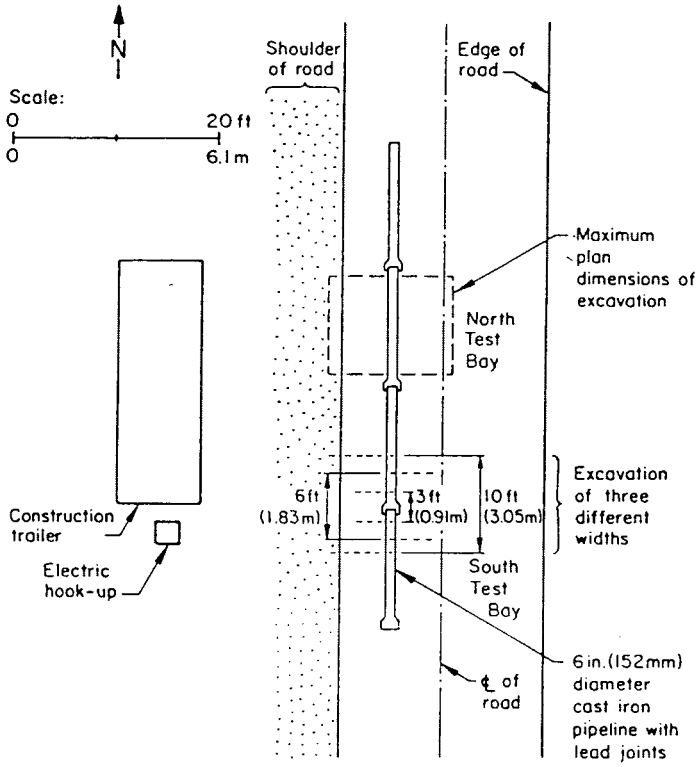

(b)

FIGURE 1 Test site layout: (*a*) profile; (*b*) plan view.

The experimental pipeline was composed of four pit cast-iron pipe segments obtained from an existing line that was installed in 1905 and taken out of service in spring 1986. Each segment had an approximate length of 3.7 m and nominal inside and outside diameters of 152 and 178 mm, respectively. The exterior diameter of the pipe was 176 mm with a standard deviation of 0.76 mm, and the pipe wall thickness was 11.3 mm with a standard deviation of 1.02 mm. The pipeline was installed with the assistance of personnel from the Brooklyn Union Gas Company in a manner consistent with the construction practices that had been used for cast-iron gas mains currently in service.

Following pipeline installation, the roadway was surfaced. The finished roadway surface consisted of a crushed limestone base course 255- to 330-mm thick covered by 75 to 100 mm of 3–2A binder.

PIPELINE INSTRUMENTATION

Field experiments and instrumentation were designed to obtain a comprehensive data set of pipeline strains generated by loads during trench construction as well as by dynamic impact loads from heavy vehicles traversing the site after the backfilling of undermining excavations. Of principal importance were the strain measurements. Other measurements included pavement surface displacement, soil settlements, stresses in the soil, temperature of the pipeline, joint rotation,

and ground and pipeline accelerations. Because of space limitations, the discussion in this paper is limited to strain gauge data. A complete description of the pipeline instrumentation and full field measurements are provided by Stewart et al. (*1*).

FIELD MEASUREMENTS

Strain gauge measurements are reported here for the test pipeline undermined by 0.9-m, 1.8-m, and 3.0-m wide trenches. For each trench width, the test pipeline was undermined by a combination of mechanical and hand excavation, generally to depths of 0.6 to 0.8 m beneath the pipe. The trench then was backfilled by loose-dumping sand. The sand was not compacted to allow the backfilling procedure to represent the worst field conditions. Crushed No. 2 stone was placed in the upper 0.3 m of the backfilled trench. A truck was then backed into specific positions along the test bay so that its wheels were directly over the pipe.

Surface loads were generated using an "overloaded" six-wheel, single rear-axle dump truck. The loads of the truck were 111.2 kN (25 kips) on the rear axle and 55.7 kN (12.5 kips) on the front axle. The suspension of the truck was not balanced, and unequal loads of 44.5 and 66.7 kN (10 and 15 kips) were measured on the left and right rear wheel sets, respectively. In addition, a 10-wheel, double rear-axle, 12.2-m^3 dump truck also was used for comparison loading conditions. The respective loads of the 10-wheel truck were 205.5 kN (46.2 kips) on the rear axle and 70.3 kN (15.8 kips) on the front axle.

Two pipeline configurations were investigated with respect to trench loads in which the wheel load was centered on (a) the middle of a pipe segment (referred to as LCP—load centered on pipe), and (b) a cast-iron joint (referred to as LCJ—load centered on joint). The LCP and LCJ configurations represent bounding conditions for response of a pipeline to localized surface load. The lead-caulked joints tend to have a low moment capacity such that the LCJ configuration is similar to a cantilever loading condition. In contrast, the LCP configuration is similar to a simply supported beam loading condition.

Figure 2 shows pipeline strains measured in response to backfilling, truck loading, and truck removal for both the LCP and LCJ configurations. The graphs are organized so that longitudinal strains averaged between the top and bottom of the pipe are plotted relative to the top chord of the pipeline. The absolute values of compressive and tensile bending strains at each gauge location were approximately equal. Average strains are plotted at each gauge station, referenced according to the distance along the pipeline. All plotted measurements are incremental strains referenced to the pipeline condition after the trench had been excavated. It was found that trench excavation tended to reduce pipeline strains to minimum values. The maximum strains in response to the truck load in each plot are for truck orientations in which the 66.7-kN (15-kip) rear wheels were positioned directly over the center of the undermined and backfilled pipeline.

Figure 3(*a*) and (*b*) show the maximum pipe strain as a function of trench width for the LCP and LCJ configurations, respectively. The increments due to backfilling and construction vehicle loading are shown along with the combined maximum strains. The peak strains in both test sections are similar in magnitude, although the locations at which they occurred are different. Peak pipe strains developed in the central portion of the test pipe for the LCP configuration. The LCJ configuration had a joint in the excavation center, resulting in maximum strains near the edges of the excavations. The maximum pipe strains due to combined backfilling and construction vehicle loading for both configurations were on the order of 200 $\mu\varepsilon$ for 0.9-m-wide trenches, 500 $\mu\varepsilon$ for 1.8-m-wide trenches, and 800 $\mu\varepsilon$ for 3.0-m-wide trenches.

THEORETICAL MODEL

Pipeline deformations caused by backfilling and construction vehicle loads, as well as by rolling and impact loads, are included in the models. The models used in this method are, by design, simple. The pipe moments computed using the models represent upper-bound predictions against which the field results are compared.

Pipeline Response to Backfilling

Figure 4(*a*) shows settlement and deformation mechanisms for the test configurations. Note that only the LCJ model contains the joint and pin. As backfill is placed on the pipe, the underlying soil compresses and moves away from the bottom of the pipe. The soil load then becomes concentrated on top of the pipe. This type of loading is analogous to a situation in which the pipeline is being lifted through the soil.

The additional load transmitted to the pipeline because of the relative movement can be characterized by a dimensionless load factor, N_v (*2*,*3*). The load imposed on the pipeline (ω), in terms of force per unit length, is given by

$$\omega = N_v \gamma Z D \tag{1}$$

where

N_v = dimensionless load factor,
γ = soil unit weight, and
Z,D = depth to pipeline centerline and outside pipe diameter, respectively.

Figure 4(*b*) shows the analogues used to calculate the strains in the pipeline, which was modeled as a pin-ended beam for the LCP configuration and as two fixed, cantilever beams connected by a hinge at the location of the joint in the LCJ configuration. The hinge cannot transfer moments. No support was considered from the poorly compacted backfill beneath the pipe. This condition was justified by stress cell readings below the invert of the pipe in the center of the LCP configuration, which showed virtually no increase in stress during the backfilling process. The effective trench width was assumed to be 0.3 m wider than the edges of the excavation to account for spalling and loosening of soil along the sides. The field data showed that the maximum strains in the LCJ configuration and the locations of zero strain in the LCP configuration were approximately 150 mm outside the edges of the trench excavation. The maximum moment (M_{max}) for both configurations, based on the conceptualized loadings

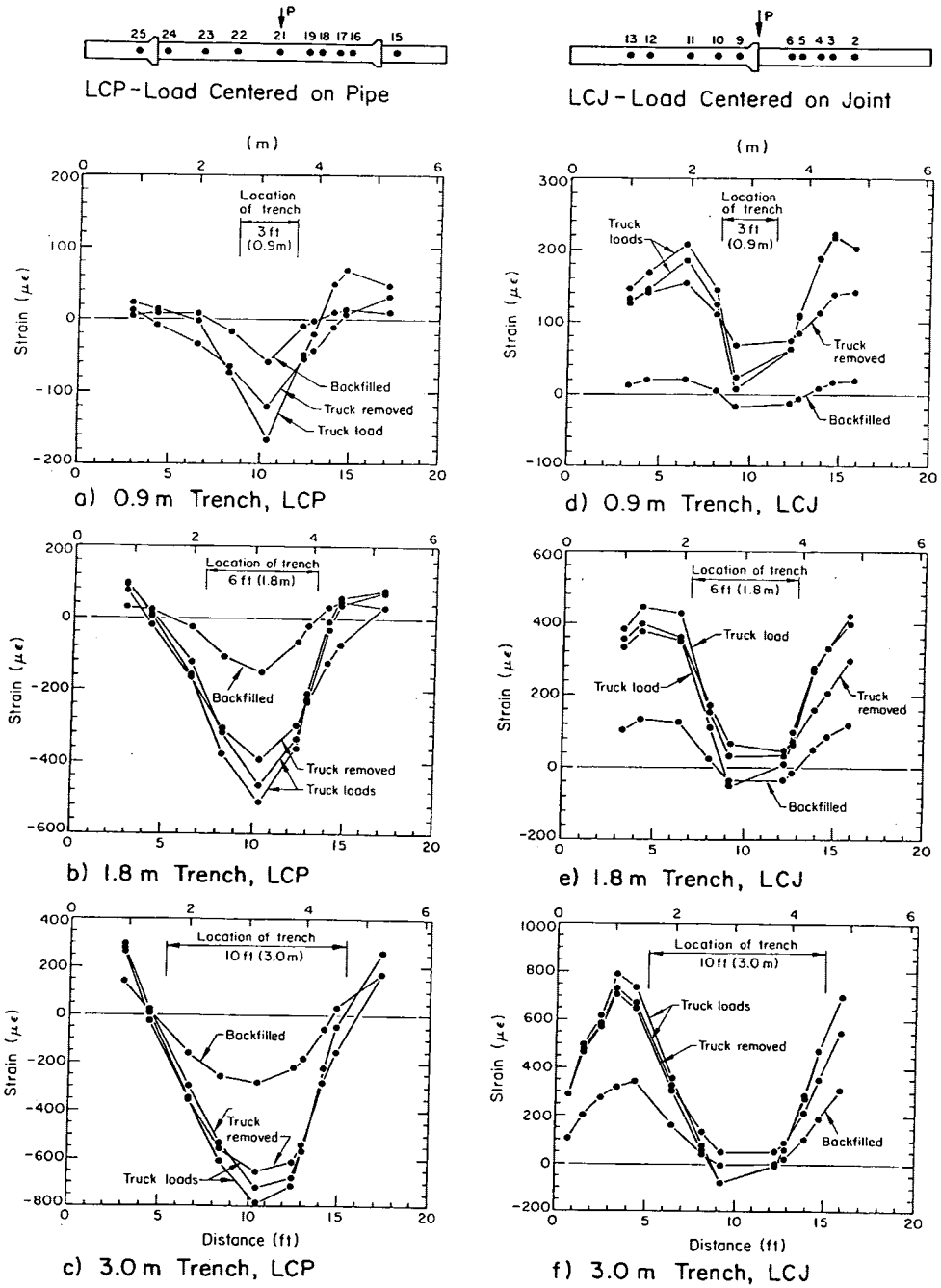

FIGURE 2 Pipeline strains measured in response to backfilling and surface loads.

shown in Figure 4(*b*), is given by

$$M_{max} = \frac{\omega \ell^2}{8} \tag{1}$$

where ω is the force per unit pipeline length and ℓ is the trench width (W) plus 0.3 m. The soil load, ω, was calculated using Equation 1 with a dimensionless load factor of $N_v = 2$ as appropriate for a loose backfill condition.

The comparisons between the maximum strains predicted by these models and those measured in the field test sections for the 3.0-m-wide trenches are shown in Figure 5. (Space limitations preclude the inclusion of comparisons for the narrower trenches.) The theoretical strains were calculated on the basis of the measured pipe geometric and material properties and soil properties described previously. In both graphs, the theoretical plots are shown by a solid curved line.

Pipeline Response to Construction Surface Loads

The strains generated by truck loads over the pipeline immediately after trench backfilling were considerably higher than those recorded during the backfilling. Figure 6 shows

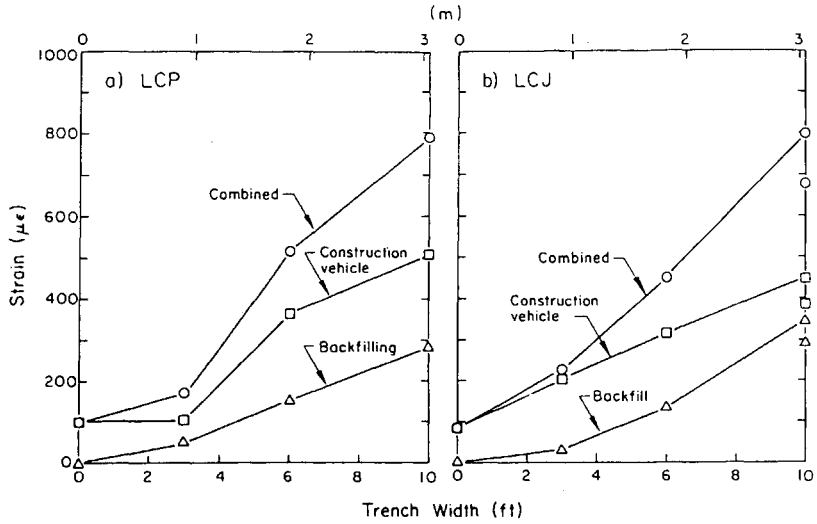

FIGURE 3 Maximum pipe strains for LCP and LCJ configurations.

the conceptual loading model for the distribution of a surface wheel load onto an underlying pipeline. A point load model (*4*) was used to evaluate the distribution of stress with depth. The locations at which the theoretical incremental stresses become negligible, on the basis of the test section geometry and predicted stresses, correspond roughly to intersections of downward-sloping lines from the surface having 1H to 1V slopes. The predicted stresses have a characteristic shape similar to that shown in Figure 6(*a*). This characteristic shape, or Boussinesq distribution, can be simplified further as a triangular stress distribution acting over a length defined by the 1H:1V projections from the surface, as shown in Figure 6(*b*).

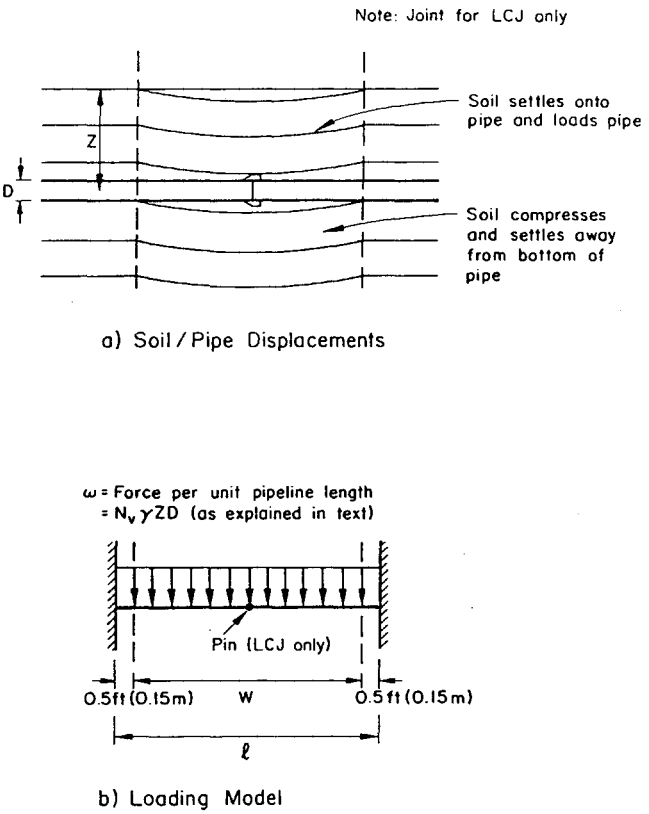

FIGURE 4 Soil/pipe displacement and loading models.

Stress cells located 75 mm above the center of the pipe in the north test bay registered stresses that were 3 to 3.5 times higher than those predicted. Measurements performed under similar conditions at the U.K. Transport Research Laboratory (*5*) have shown that the vertical stress distribution was more sharply peaked and approximately 1.9 times greater than that predicted by elastic theory.

There is theoretical justification for the increased level of stress. Backfill settlement and compaction during surface loading increase the backfill density from a loose to medium-dense condition. The increased density results in additional friction load, which should be consistent with a dimensionless load factor (N_v) of 3 for medium-dense granular soil (*2,3*). The stress cell recordings showed vertical soil loads in agreement with the theoretical load factor. A triangular stress distribution was therefore assumed with a base length equal to 1.50 m (two times the depth to the crown of the pipe) and a peak stress equal to three times that predicted by the point load Boussinesq-type distribution.

A simply supported beam analogue of this loading condition is shown in Figure 6(*c*). For most conditions, this model overpredicts the pipeline strains when compared with field measurements and does not account properly for the distribution of pipeline strains beyond the sides of the undermining trench. Although this type of model is helpful in setting an upper bound on pipeline response, additional refinements were needed to develop a more robust model for analytical predictions.

The pipe test sections were modeled as partially supported beams on elastic foundations, with the backfill providing support beyond the triangular load distribution. The soil reaction is characterized in Figure 6(*b*) as a series of springs on either side of the undermining trench. The subgrade reaction zones were modeled as short, pin-ended truss elements with a spring stiffness equal to a coefficient of subgrade reaction.

The coefficients of subgrade reaction (k_s) were derived from bearing capacity analyses and considerations of the pipe dis-

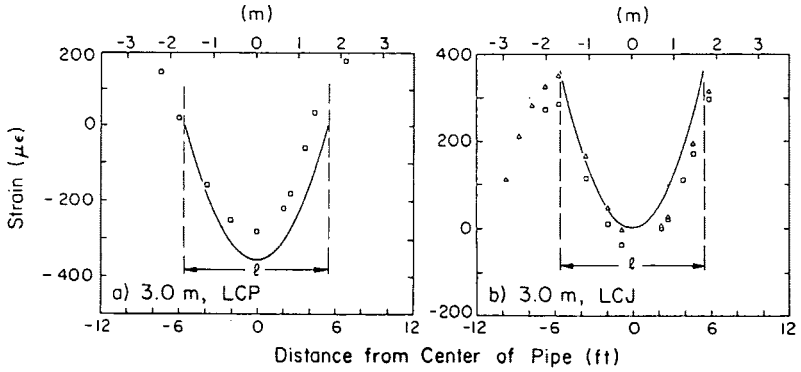

FIGURE 5 Measured and predicted pipe strains, 3.0-m trench.

placements. The values used for loose and dense backfill were k_s = 2270 and 22 500 kN/m², respectively. These values fall within those given by (*6*), which are in the range of 1090 to 3280 kN/m² for loose fill, and 16 400 to 54 700 kN/m² for dense fill.

Because the trench excavations were symmetrical about the trench centerlines, only half of the pipe geometry and support conditions required modeling. A schematic of the beam on elastic foundation (BOEF) model used for the 3.0-m trench excavations is shown in Figure 7. Details of the narrower trench excavation models are given by Stewart et al. (*1*). For the LCP pipe sections, a pipe joint element was placed 1.8 m from the trench centerline. A pipe joint element also was placed at the trench centerline for the LCJ configuration. The influence length for the triangular stress distribution extended 0.75 m on either side of the trench centerline. The equivalent reaction spring stiffnesses beyond the excavation limits and 150-mm loosened soil zones were those corresponding to dense soil. Spring stiffnesses based on a loose soil support condition were placed beneath the pipe within the excavation limits and the loosened soil zones. Short beam sections (25 mm) were used to model the lead-caulked joints and were given a bending stiffness (EI) of 1 percent of the pipe bending stiffness.

The comparisons between the measured pipeline strains in the north test bay and those computed using the BOEF models are shown in Figure 8. The BOEF model predictions were in good agreement with the measured strains. The critical strain locations for the LCJ configuration occur near edges of the trenches, and the strains are shown as tensile on the pipe crown.

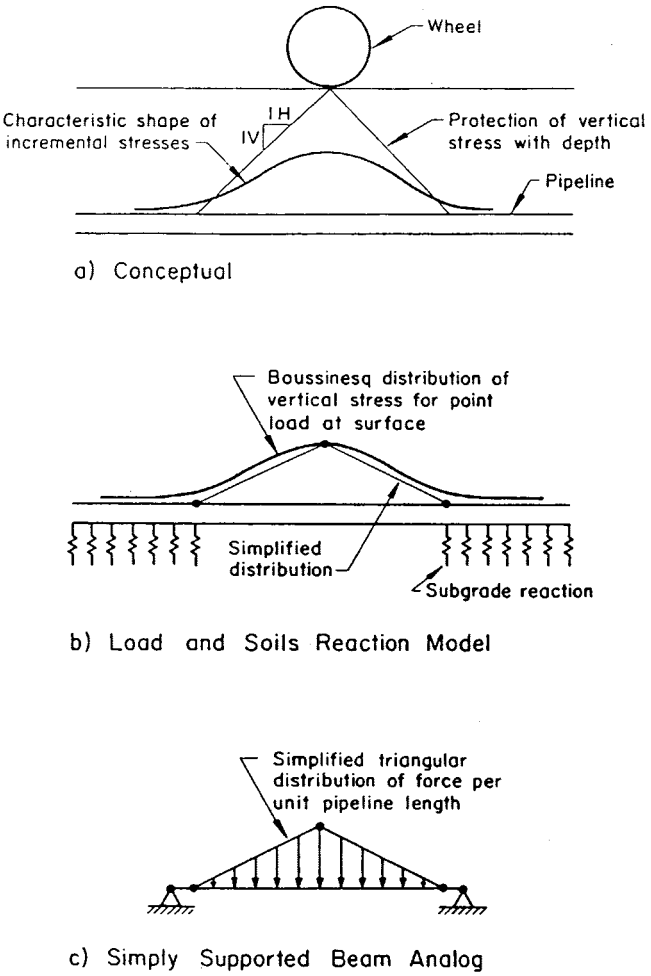

FIGURE 6 Vertical stress transfer from vehicle loads.

Combined Soil and Construction Vehicle Loading

The strains due to trench backfilling followed by construction vehicle loading are the algebraic sum of the strains for each of the two phases. The maximum strains due to trench backfilling are shown in Figure 9(*a*).

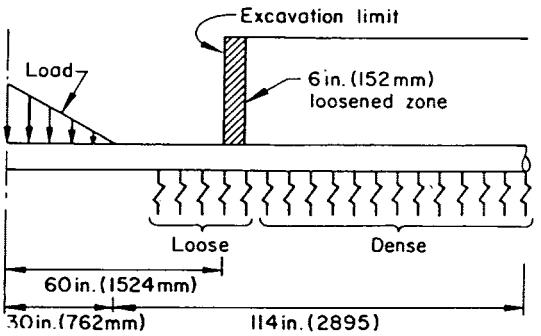

FIGURE 7 Generalized BOEF model used for characterizing vehicle loadings, 3.0-m trench.

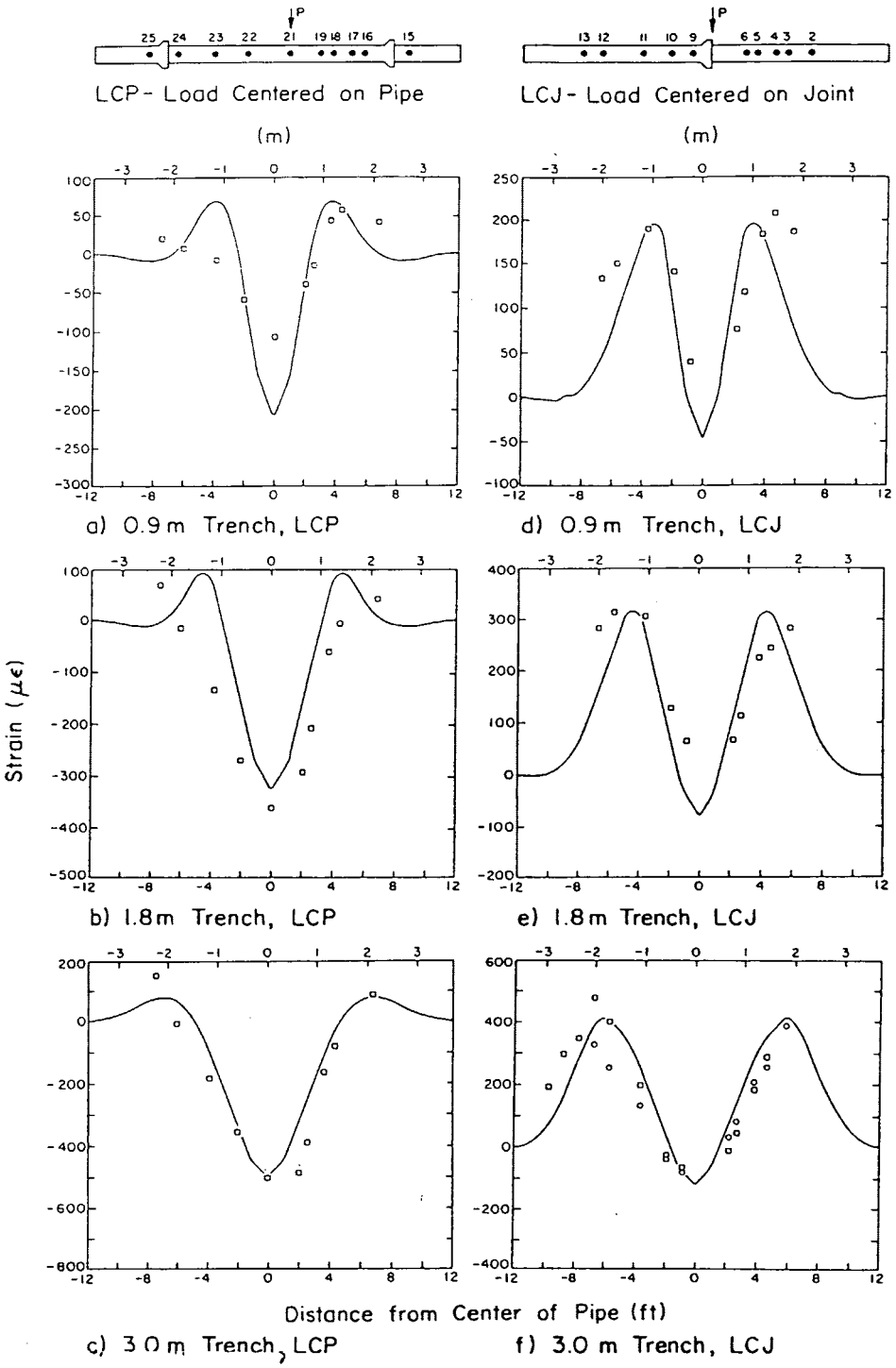

FIGURE 8 Measured and predicted strains due to vehicle loading.

Figure 9(*b*) shows the maximum pipeline strains due to construction vehicle loading only, which are dependent on trench width. The graph shows the predicted strains based on the simple beam model as well as the more refined BOEF models for both pipeline configurations. For trench widths up to 1.8 m, the simplified model appears reasonable; however, it is overly conservative for trench widths beyond 1.8 m, and the BOEF models result in better agreement between the predicted values and those measured in the field tests.

Analyses indicated that there is a trench width beyond which the vehicle-induced strains no longer increase. This limiting trench width is on the order of 2.7 to 4.6 m. Trench widths greater than this could result in entire 3.7-m-long pipe sections lying between the excavation limits. Because the joints transfer little moment, the effective pipe length over which moments would develop would be controlled by the length of the pipe sections between the nearest exposed joint and the edge of the excavation.

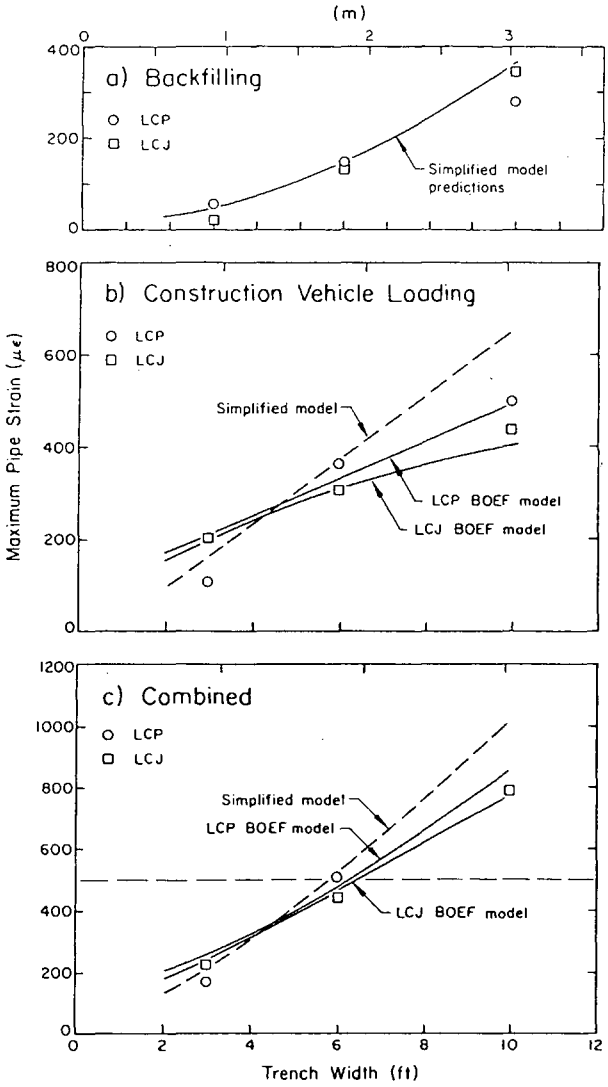

FIGURE 9 Maximum pipeline strains.

The strains resulting from combined backfill and surface vehicle loading are shown in Figure 9(*c*). These maximum strains were obtained by adding the maximum measured and predicted strains from the two separate cases. It should be recognized that the field data and analytical model predictions represented in this graph cover the worst, or upper-bound, loading conditions in the field. The measured and predicted pipe responses both show that 500 με is exceeded for trenches greater than 1.8 m wide. In addition, the simplified loading models give reasonably accurate and conservative results for trench widths in the range of 0.9 to 1.8 m.

COMBINED STATIC AND DYNAMIC LOADING

Factors that must be considered in addition to those generated by backfilling and construction vehicle loading are the strains due to the impact of traveling surface traffic following pavement resurfacing. Rolling-wheel loads and impacts caused by surface irregularities were considered for pipeline loading. A complete description of the dynamic tests is given elsewhere (*1*), and only a brief treatment of the primary results is provided here. Impact conditions in the dynamic tests were represented by an uneven roadway and various surface obstructions with dimensions similar to those associated with temporary asphalt patching of streets. Vehicle speeds ranged roughly between 14.5 and 53.0 km/hr.

The average rolling-wheel load strain in the LCP configuration was roughly 88 ± 14 με and for the LCJ configuration, 67 ± 18 με. The combined average rolling-wheel load strain developed in both test sections for the types of surface irregularities used in the rolling-wheel tests was 79 ± 19 με. An upper limit, then, to be used in the impact design methodology for a rolling-wheel load, was taken as 100 με (79 + 19 ≈ 100). This strain level compares favorably with the values reported for similar bedding conditions (*7,8*).

Average impact factors were calculated as the ratio of strain with impact divided by the average strains under static loading conditions. The combined average impact factor for these data was 1.42 with a standard deviation of 0.24. The impact factor that was selected for use in the impact formulation presented here was 1.65, which is roughly equivalent to the combined average of 1.42 plus one standard deviation of 0.24. This impact factor is consistent with other recommendations (*9,10*).

The final result of these quasi-static rolling-wheel loads and measured dynamic impact factors can be used to estimate a reasonable upper bound of expected dynamic strains. For the field test sections then, an expected dynamic strain would be calculated at 165 με, which is the product of the upper-bound rolling-wheel increment of 100 με multiplied by the upper-bound dynamic impact factor of 1.65.

The field experiments were conducted for a 0.75-m burial depth. However, mains may be found in the depth range of 0.6 to 1.5 m. For pipelines buried deeper than 0.75 m, the dynamic stress increments would be reduced, resulting in decreased dynamic strains. For this design methodology, the stresses predicted using the point load model (*4*) at depths from 0.6 to 1.5 m were normalized by the predicted stresses at a depth of 0.75 m. The dynamic strains at other depths were then predicted relative to the strains at 0.75-m depth multiplied by the normalized stresses for the given depth. Thus, the incremental dynamic strains at a depth of 0.6 m would be approximately 1.5 times greater than the strains at 0.75 m. Likewise, the expected strains at a depth of 1.1 m would be roughly one-half of those at a depth of 0.75 m. The rolling-wheel load strains at depths then are estimated by using the 100 με upper bound, measured in the field experiments at 0.75-m depth, and the appropriate stress ratio. For the previous example depths of 0.6 and 1.1 m, this would result in rolling-wheel strains of 150 and 50 με, respectively.

The final step in determining pipeline strains must consider all contributors, that is, backfill loading, construction vehicle loading, and dynamic traffic-induced strain. Because the residual strains following unloadings of the construction vehicles were on the order of 75 to 90 percent of the peak strains under load, no reduction in backfill and construction vehicle-related strains was considered, which adds a reasonable level of conservatism to the design methodology. The total allowable pipeline strain has been limited to 500 με. Because the dynamic strain decreases with increasing depth, the backfill and construction vehicle-related strains can be a greater percentage of a total allowable design strain of 500 με as pipe burial

depth increases. Parametric studies were performed to determine the expected pipe strains as a function of trench width for 102-, 152-, and 203-mm pit cast-iron mains at various burial depths ranging from 0.6 to 1.5 m. Complete details are provided by Stewart et al. (*1*).

RECOMMENDATIONS FOR PRACTICE

The methodology given here has been followed for 102-, 152-, and 203-mm nominal pipe diameters. Figure 10 shows the maximum trench widths as dependent on a depth of burial that would result in a 500-με pipe strain. As the depth of burial increases from 0.6 to 1.5 m, the maximum trench width increases but reaches limiting values. At typical minimum depths of 0.75 m, the maximum trench widths would be approximately 0.9, 1.2, and 1.7 m for 102-, 152-, and 203-mm diameter mains, respectively. At burial depths of 1.2 m or more, the maximum trench widths would be limited to approximately 1.2, 1.8, and 2.4 m for pipes having diameters of 102, 152, and 203 mm, respectively.

The design chart shown in Figure 10 is based on several observations that require additional interpretations. As trench width increases, the pipe-unsupported span increases, resulting in higher backfill-related strains as well as increased strains caused by construction vehicle loading. The combined effect is that pipeline strains increase for constant burial depth as the trench width increases. For constant pipe burial depth, two interactions must be considered. The backfill-related strains increase as the depth of burial increases. However, the imposed construction vehicle load and resulting pipe strains decrease as burial depth increases. At depths larger than roughly 1.2 m, the increase in backfill strains is compensated for by the decrease in construction vehicle strain, resulting in, for constant trench width, about the same level of combined pipe strain.

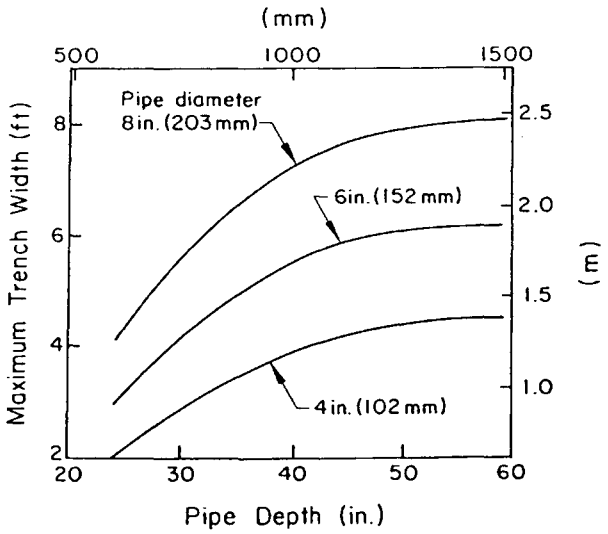

FIGURE 10 Maximum trench width versus pipe depth.

CONCLUSIONS

Field tests were conducted to evaluate the static and dynamic responses of cast-iron mains undermined by perpendicular excavations. A 14.6-m long instrumented pipeline was installed using four 3.7-m lengths of 152-mm nominal diameter pit cast-iron pipe sections with lead-caulked joints. Excavations of 0.9, 1.8, and 3.0 m widths were made, centered on a lead-caulked joint and also at the middle of a pipe section. A poorly graded, coarse-to-medium sand was used as backfill. This type of backfill is similar to materials commonly used in pipeline construction, particularly urban excavations. Pipeline strains were measured due to backfilling and construction vehicle loading and under impact conditions. Analytical models were developed on the basis of the field test results to evaluate pipe strains due to excavation crossings.

Pipe strains due to backfilling and construction vehicle loading increased as trench width increased for both test sections. The locations of maximum pipe bending strains in the LCP configuration were in the mid-portion of the pipe in the center of the excavation. In the LCJ configuration, the excavations were centered on a pipe joint, and the maximum strains occurred near the excavation margins.

Simple beam models were developed, along with more complete BOEF-type solutions. The simple beam models accurately predicted the strain measured in the pipeline for the 0.9- and 1.8-m excavations, but were overly conservative for 3.0-m trenches. The BOEF models accurately predicted the pipeline response for all trench widths.

The final design recommendations were based on a combination of static and dynamic effects. Design recommendations for maximum excavation width and a limiting strain of 500 με were presented and considered the effects of pipe diameter and burial depth. For typical minimum burial depths of 0.75 m, the maximum allowable trench widths would be 0.9, 1.2, and 1.7 m for 102-, 152-, and 203-mm diameter mains, respectively. At burial depths of 1.2 m or more, the maximum trench width would be limited to 1.2, 1.8, and 2.4 m for pipes having diameters of 102, 152, and 203 mm, respectively.

ACKNOWLEDGMENTS

The work presented in this paper was performed as part of research sponsored by the New York Gas Group (NYGAS). Appreciation is extended to Robert B. Meade, the NYGAS RD&D Program Manager and Contract Administrator, and to George M. Kok and Arthur A. Shapiro, Project Managers from Brooklyn Union Gas Company. Thanks are extended to B. J. O'Rourke, K. M. Kohl, B. M. New, and I. Ahmed for their participation in the work. A. Avcisoy and K. J. Stewart, who prepared the drawings and the manuscript, respectively, are duly recognized for their skills and contributions.

REFERENCES

1. Stewart, H. E., B. J. O'Rourke, and T. D. O'Rourke. *Evaluation of Cast Iron Response at Excavation Crossings*. Geotechnical Engineering Report 89-1. School of Civil and Environmental Engineering, Cornell University, Ithaca, N.Y., Jan. 1989.

2. Trautman, C. H., and T. D. O'Rourke. Behavior of Pipe in Dry Sand Under Lateral and Uplift Loading. *Geotechnical Engineering Report 83–7*. School of Civil and Environmental Engineering, Cornell University, Ithaca, N.Y., May 1983.
3. Trautman, C. H., T. D. O'Rourke, and F. H. Kulhawy. Uplift Force-Displacement Response of Buried Pipe. *Journal of Geotechnical Engineering*, ASCE, Vol. 111, No. 9, Sept. 1985, pp. 1061–1067.
4. Carder, D. R., P. Nath, and M. E. Taylor. *A Method of Modeling the Effect of Traffic on Undermined Buried Pipelines*. Laboratory Report 1028. U.K. Transport and Road Research Laboratory, Crowthorne, Berkshire, England, 1981.
5. Crabb, G. I., and D. R. Carder. *Loading Tests on Buried Flexible Pipes to Validate a New Design Model.* Research Report 28. U.K. Transport and Road Research Laboratory, Crowthorne, Berkshire, England, 1985.
6. Terzaghi, K. Evaluation of Coefficients of Subgrade Reaction. *Géotechnique*, Vol. 5, No. 4, Dec. 1955, pp. 297–326.
7. Pocock, R. G., G. J. L. Lawrence, and M. E. Taylor. *Behavior of a Shallow Buried Pipeline Under Static and Rolling Wheel Loads.* Laboratory Report 954. U.K. Transportation and Road Research Laboratory, Crowthorne, Berkshire, England, 1980.
8. Taylor, M. E., G. J. L. Lawrence, and D. R. Carder. *Behavior of a Shallow Buried Pipeline Under Impact and Abnormal Loads.* Laboratory Report 1129. U.K. Transport and Road Research Laboratory, Crowthorne, Berkshire, England, 1984.
9. *Recommended Practice for Liquid Petroleum Pipelines Crossing Railroads and Highways.* API Recommended Practice 1102, 6th ed. American Petroleum Institute, 1992.
10. Committee on Pipeline Crossings of Railroads and Highways. *Interim Specifications for the Design of Railroads and Highways.* American Society of Civil Engineers, New York, 1964.

Publication of this paper sponsored by Committee on Subsurface Soil-Structure Interaction.